ULTRASOUND BEHAVIOR OF DIFFERENT CERAMIC PIEZOELECTRIC TRANSDUCERS APPLIED TO SONOLUMINESCENCE[1]

A.L.F. de Barros[2]
G. Watanabe[3]
A.L.M.A. Nogueira[4]
R. Lopes[5]

Abstract: Single-bubble sonoluminescence (SBSL) is a light-emission event from a stably oscillating bubble trapped at the pressure anti-node of a standing ultrasound wave, a phenomenon that has been studied intensively for a decade [1]. Using ceramic piezoelectric transducers PZT, we are able to irradiate a liquid inside a resonator flask by means of an ultrasound wave, and we eventually capture a bubble inside a restricted domain in the aqueous medium. The trapped bubble will expand and collapse at an accelerated rate, emitting light. To capture the bubble we perform some experiments using differently sized and shaped piezoelectric transducers, and we manage to verify their capacitance and impedance behavior in our sonoluminescence circuit. Our experiments were performed at Laboratory of Experimental and Applied Physics (LaFEA) at CEFET-RJ.

Keywords: light emission, sonoluminescence, PZT, ultrasound.

1. INTRODUCTION

Sonoluminescence (SL) is one of the most fascinating phenomena studied in the past few years. It may be the world's most nonlinear oscillator as well as the world's most effective means of spontaneously focusing energy [2]. To reproduce the phenomenon of SL we need to implement a certain frequency (range of 20 kHz to 35 kHz), called resonance frequency. This frequency will be applied in the resonator, which is a quartz flask container filled with the liquid medium that will be irradiated [3].

Fig. 1 illustrates a typical experimental setup for generating SBSL. A piezoelectric synthesizer drives PZT's, mounted to a water-filled acoustic levitation cell, is driven to set up a standing wave within the water. The drive frequency depends on the size and geometry of the levitation cell or resonator (which can be spherical, cylindrical, or even rectangular) [4]. The water is typically degassed to about 10% of saturation. A bubble is introduced by injecting air through a syringe into the water. The bubbles rise to the surface, while the small bubbles are attracted to pressure antinodes. The final size of the remaining bubble at the antinode depends on gas diffusion steady state conditions and instabilities present: if the bubble is too small, gas will transport into the bubble; if the bubble is too large, small micro bubbles will be ejected from the main bubble. In this manner, the final bubble comes into a diffusive steady state. Once the bubble is positioned at the pressure antinode, the drive pressure amplitude is increased until sonoluminescence is observed [5].

[1] Departamento de Disciplinas Básicas e Gerais - Centro Federal de Educação Tecnológica Celso Suckow da Fonseca-CEFET-RJ, Av. Maracanã 229, 20271-110 - Rio de Janeiro.
[2] Ana Lucia Ferreira de Barros - abarros@cefet-rj.br
[3] Gabriel Watanabe - watanabe01@gmail.com
[4] Álvaro Luis Martins de Almeida Nogueira - almanogueira@gmail.com
[5] Rafael Pereira Lopes - rafap16@hotmail.com

Figure 1 - Basic experimental scheme, a function generator, an amplifier, the variables coils, the resonator and the piezoelectric (PZT), and, in addition, the oscilloscopes

In this work, we calculate the variation of the inductance and the capacitance when the bubble was captured for a variety of PZT's. Therefore, knowing the resonant frequency and the above mentioned data we are able to match sonoluminescence.

Table 1 - Specifications of the piezo-electric transducer

Types of Resonators	Volume (ml)	Types of PZT	PZT Dimensions (mm)	Curie Temperature (°C)	Dielectric Constant (nF/m)[a]	Capacitance (nF)[b]	Indutance (μH)[c]
Spherical	100	PIC140	10.0 x 1.0	330	1200	1668.0	0.23
Spherical	250	PIC141	15.0 x 3.0	275	1300	1355.2	0.28
Spherical	100	PIC155	18.0 x 4.0	345	1500	1688.8	0.23
Cylindrical	100	PIC 151	20 x 10 x 4	250	2100	1167.6	0.33

[a] Datasheet of your transducers [6].

[b] $C = \frac{13.9ed^2}{h}$ where d is the diameter, h is the thickness and e is the dielectric constant of a transducer .

[c] $L = \frac{1}{C(6.28\,f)^2}$ where f is the resonance frequency (calculated by Eqn. (17)).

2. MATERIAL USED

To trigger SL, we will use a sine wave audio generator; a power amplifier (40 W ~ 1500 W); piezoelectric transducers (specified at Table 1); resonance quartz chamber; inductors (10 to 40 mH); oscilloscopes; a multi-meter. We use four kinds of small necks resonators, as shown in figure 2, with different PZTs sizes attached on them.

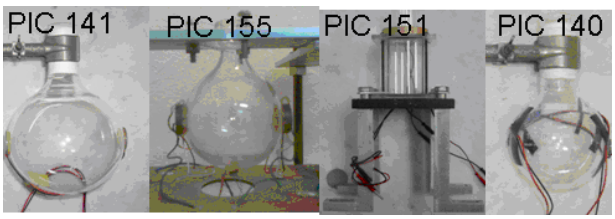

Figure 2 - The photography of the cylindrical and spherical resonators flasks at 100 ml and 250ml

The resonance chamber is a simple open ended Plexiglas chamber. Depending on shape or size, a corresponding resonant frequency is to be matched. Conversely, one of the technical problems in generating sonoluminescence is providing a chamber that will resonate at a very specific accessible frequency. We are working with two different kinds of resonators: spherical and cylindrical. The mathematical approach that we now present is meant to roughly indicate how to select the frequency in the given resonator and how to obtain the phenomenon.

The general wave form is a solution to the following equation:

$$\nabla^2 f = \frac{1}{c^2}\frac{\partial^2 f}{\partial t^2} \quad (1)$$

This is known as the wave equation which relates the Laplacian operator of a function that is dependent upon x, y, z and t, to a second partial derivative of the function with respect to t. The proportionality constant relating the 2nd spatial derivative to the 2nd time derivative determines the speed of the wave (c). In order to solve the wave equation, we assume the solution to be variable separable:

$$f(x,t) = X(x)Y(y)Z(z)W(t) \qquad (2)$$

Plugging Eqn.(2) into the wave equation, Eqn.(1), leads to Eqn.(3). Putting apart time and spatial dependence on opposite sides of the equation leads to:

$$c^2\left[\frac{1}{X(x)}\frac{d^2X(x)}{dx^2}+\frac{1}{Y(y)}\frac{d^2Y(y)}{dy^2}+\frac{1}{Z(z)}\frac{d^2Z(z)}{dz^2}\right]=\frac{1}{W(t)}\frac{d^2W(t)}{dt^2} \quad (4)$$

The left side of this equation only depends on X, Y and Z while the right side only depends on W. Therefore, we conclude that both sides of the equation are equal to a constant $-\omega^2$. For the time being, we are only concerned with the position dependent term and the time dependent term can be disregarded. Rearranging Eqn.(4) and, for convenience, introducing a new constant k_n given by Eqn.(5), we have:

$$k_n^2 = \frac{\omega^2}{c^2} \qquad (5)$$

$$\frac{1}{X(x)}\frac{d^2X(x)}{dx^2}+\frac{1}{Y(y)}\frac{d^2Y(y)}{dy^2}+\frac{1}{Z(z)}\frac{d^2Z(z)}{dz^2}=-k_n^2 \quad (6)$$

As we take $k_n^2 = k_x^2 + k_y^2 + k_z^2$, we may further rearrange Eqn. (6) to isolate the differential for each coordinate, arriving at:

$$\frac{d^2X(x)}{dx^2} = -X(x)k_x^2 \qquad (7)$$

From Eqn.(7) we obtain a function whose second spatial derivative is proportional to the function itself, with a relative sign change. The general solution for this type of differential equation is given by:

$$X(x) = A\cos[k_x x] + B\sin[k_x x] \qquad (8)$$

Once the general solution to the wave function has been obtained, the boundary conditions must be considered. We set up a system where the wave is confined in the region $0 < X < L_x$, exhibiting nodes at the boundary points. Consequently, the cosine term drops out and we get the constant k_x constrained in such a way that when x equals L_x, the term within the sine function will be an integer times ϖ, making the sine term equal to zero at $X = L_x$.

The positive integer N_x corresponds to the number of anti-nodes (Fig. 3). For the confined wave pattern, every wave must present at least one anti-node and therefore N_x is not allowed to equal zero.

$$\frac{d^2X(x)}{dx^2} = -X(x)k_x^2 \qquad (9)$$

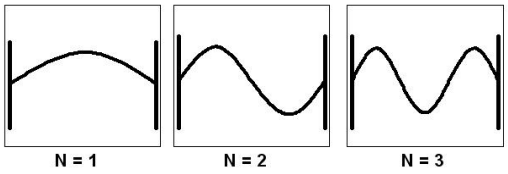

Figure 3 - Description of the positive integer N_x =1 to 3; N_x is regarded as a counter for the number of anti-nodes exhibited by the corresponding wave mode

The wave solution then becomes:

$$X(x) = B\sin[\frac{N_x \pi x}{L_x}] \qquad (10)$$

Solving the above equation for the resonant frequency for this type of wave:

$$N(\frac{\lambda}{2}) = L \qquad (11)$$

$$c = f_{res}\lambda \qquad (12)$$

$$f_{res} = \frac{Nc}{2L} = \frac{cN\pi}{2\pi L} = \frac{c}{2\pi}k \qquad (13)$$

The Resonant frequency for a standing wave in a rectangular cell:

$$f_{res}(N_x, N_y, N_z) = \frac{c}{2\pi}\sqrt{k_x^2 + k_y^2 + k_z^2} \qquad (14)$$

Here c stands for the speed of sound through water and N stands for the number of nodes in the x, y and z directions. Only one node is needed in each direction; however we

chose N_Z to be 2 for future studies in multi-bubble SL [7].

For the cylindrical cell, a similar argument can be used, this time in (r, ϕ) coordinates (we use ϕ rather than θ here because of its parallel role in the spherical case, to be discussed shortly).

The wave equation in polar coordinates can be written:

$$\frac{1}{r}\frac{\partial}{\partial r}r\frac{\partial f}{\partial r}+\frac{1}{r^2}\frac{\partial^2 f}{\partial \varphi^2}=\frac{1}{c^2}\frac{\partial^2 f}{\partial t^2} \qquad (15)$$

Separation of variables gives a radial equation called Bessel's equation; the solutions are called Bessel functions [8]. The boundary conditions that represent the confinement of wave modes inside the cylindrical resonator impose a null solution for r = a - radius of the cylinder - and for two values of z, z = 0 and z = L, say, locating on the "caps" of the cylinder. As commented on for rectangular symmetry, the boundary conditions shall lead to a discrete spectrum and a corresponding set of resonant frequencies.

Finally, let us consider elastic waves on the surface of a sphere, such as an inflated spherical bubble. The natural coordinate system here is spherical polar coordinates, with θ measuring latitude, but counting the North Pole as zero, the South Pole as ϖ. The angle ϕ measures longitude from some agreed origin.

The wave equation in spherical coordinates can be written:

$$\frac{1}{\sin\theta}\frac{\partial}{\partial\theta}\sin\theta\frac{\partial f}{\partial\theta}+\frac{1}{\sin^2\theta}\frac{\partial^2 f}{\partial\varphi^2}=\frac{r^2}{c^2}\frac{\partial^2 f}{\partial t^2} \quad (16)$$

Again, this wave equation is solved by separation of variables. The time-independent solutions are called the Legendre functions [9]. They are the basis for analyzing the vibrations of any object with spherical symmetry. Eventually, one should impose the boundary conditions that represent the confinement of wave excitations inside the resonator, leading to a null value of the solution for r = a, where a is the radius of the sphere. Again, a discrete collection of standing modes defines the set of resonant frequencies.

3. EXPERIMENTAL PROCEDURE

A function generator is needed to supply the correct frequency for the apparatus and, as the initial source of power; it has to ensure a high level of precision. Due to the strong sonic pressure needed for this experiment, an audio power amplifier is used to boost the signal from the function generator of 250 W or internal impedance matching capabilities.

The PZT is made up of a special type of ceramic which, when an AC voltage is applied to it, will expand or contract depending on the direction of current through the ceramic. Thus, it will generate a sound wave. Conversely, from a varying pressure mode income we obtain an electrical signal. As a result of this physical property, we use PZT like the driving element of the system when attached to a resonator or being used as a hydrophone, on the top of the resonator. Attaching the PZT to the resonator can be a hard task to cope with. Every PZT presents a critical temperature known as a Curie point at which the ceramic will depolarize and no longer preserve its functional properties. These temperature values are described in table 1.

Another fact that should be observed while working with piezoelectric transducers is their parasite effects. Examining the equivalent circuit of the PZT manufacturers, we verified that the predominant effect in our experimental setup is the capacitive one, which can cause a great loss in power on the system. As we need a higher voltage and current, it is important to avoid this loss without damaging the circuit [10]. Therefore, we construct an alternative RLC circuit which makes the inductor cancel the capacitive reactance.

4. MATCHING THE CAPACITANCE AND THE IMPEDANCE

The PZT acts like a very inefficient capacitor. This capacitor has some impedance that will take power away from the rest of the system. To minimize this problem, an inductor must be inserted to cancel out this impedance, as in a basic RLC circuit.

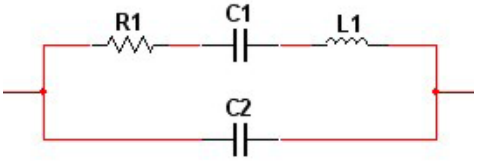

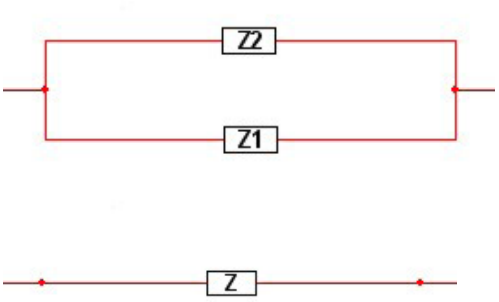

Figure 4 - The impedance circuit of the two PZT´s attached to the resonators. Z is the equivalent impedance of Z_1 and Z_2

In order to maximize the power output of the apparatus, the resonant frequency of the RLC circuit must match the other resonant frequencies. The amount of inductances (L) needed for the circuit board can be calculated from the known resonant frequency, Eqn.(17), and the capacitance (C) of the PZT (table 1):

$$f_{res} = \frac{1}{2\pi\sqrt{LC}} \quad (17)$$

The main idea of our measurement is to analyze the behavior of the PZT that is connected to the resonator. Therefore, we need to determine the PZT capacitance and the impedance of the system following the frequency variation, until the phase is matching. For the capacitance measurements, we fixed a value for the frequency and changed the value of inductance to match the resonance. Knowing the inductance we can calculate the capacitance value using Eqn.(17). For the impedance measurements, we have two possible strategies to adopt:

1) Knowing the values of C_1, C_2, L_1 and R_1 (Fig. 4), we can calculate the impedance Z as follows:

$$Z_1 = R_1 + i\left(X_{L_1} - X_{C_1}\right)$$
$$X_1 = \left(X_{L_1} - X_{C_1}\right)$$
$$Z_2 = -iX_{C_2}$$

$$Z = Z_1 // Z_2 = \frac{Z_2 Z_1}{Z_2 + Z_1} = \frac{-\left(R_1 + iX_1\right)iX_{C_2}}{R_1 + i\left(X_1 - X_{C_2}\right)}$$
$$= \frac{\left(X_1 X_{C_2}\right) - \left(iX_{C_2} R_1\right)}{R_1 + i\left(X_1 - X_{C_2}\right)}$$

$$= \frac{\left(+X_1 X_{C_2} - iX_{C_2} R_1\right)\left(R_1 - i(X_1 - X_{C_2})\right)}{R^2{}_1 + (X_1 - X_{C_2})^2}$$

$$\frac{{}_{C_2} R_1\left(X_1 - X_{C_2}\right) + X_1 X_{C_2} R_1\right] - i\left[X_1 X_{C_2}\left(X_1 - X_{C_2}\right) +}{R_1{}^2 + \left(X_1 - X_{C_2}\right)^2}$$

$$= -X_{C_2}\left[\frac{-R_1 X_{C_2} + i(X_1(X_1 - X_{C_2}) + R_1{}^2)}{R_1{}^2 + (X_1 - X_{C_2})^2}\right.$$

$$_{C_2} \frac{R_1 X_{C_2} - i\left[R_1{}^2 + \left(X_{L_1} - X_{C_1}\right)\left(X_{L_1} - X_{C_1} - X_{C_2}\right)\right]}{R_1{}^2 + \left(X_{L_1} - X_{C_1} - X_{C_2}\right)^2} \quad (18)$$

C_1 is the material elasticity, C_2 is capacitance between the terminals, L_1 is the vibrational mass of the quartz and R_1 is the intrinsic loss of the system.

2) Building the circuit sketched in Fig. 5; to obtain the impedance values we fixed the frequency and voltage in the circuit and we varied the resistance to accomplish in the two channels of the oscilloscopes until the voltage in the circuit drops to half the original value. This means that the resistor had the same impedance as the PZT. In Fig. 5, XFG1 is the function generator; U_1 the amplifier, XSC1 the oscilloscope, while R_2 is an adjustable resistance to the amplifier gain and R_1 is a resistive decade from which the module of impedance and resistance can be read. The R_1 ranges from the 0Ω to 1MΩ with step of 1Ω and error of 0.5% per resistor. Also, X_1 is the equivalent C_1 and C_2 PZT´s attached to the resonator.

For the capacitance behavior, we constructed the experimental setup of Fig. 6, and we varied the frequency until the phase is matching. In Fig. 6, XFG1 is the function generator; U_1 the amplifier, XSC1 the oscilloscope, while R_1 = 1 Ω R_2 = 1 MΩR_3 = 10 kΩ and R_4 varies from 1 Ω to10 Ω resistances employed to control the amplifier power and L_1 varies from 10 to 40 mH. Also, X_1 is the equivalent C_1 and X_2 the C_2 PZT´s attached to the resonator.

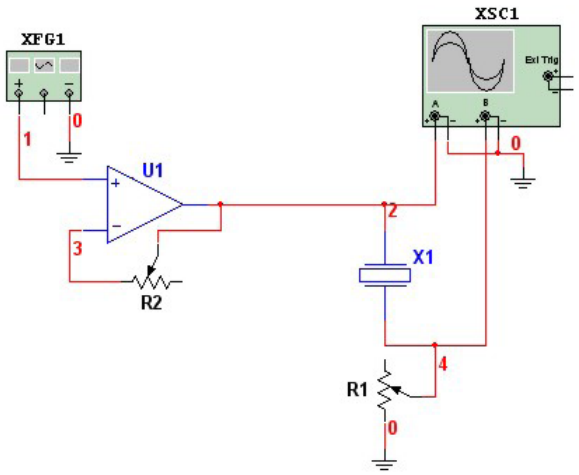

Figure 5 - The experimental setup to determine the PZT impedance module versus the frequency until the phase matching

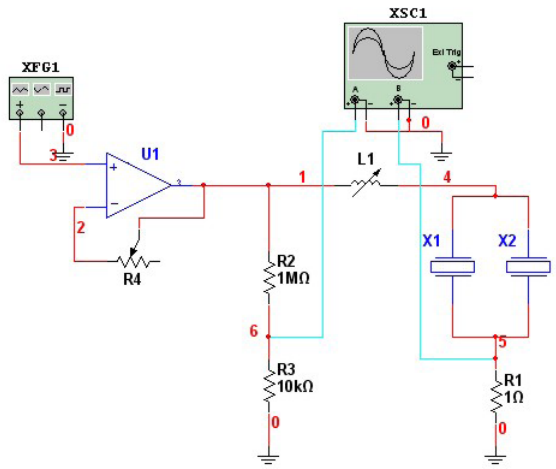

Figure 6 - The experimental setup to determine the PZT capacitance versus the frequency until the phase matching

5. RESULTS

The idea of the SL apparatus is to create a three dimensional acoustic standing wave inside a resonance chamber strong enough to trap a single bubble at a known position and force it to collapse [11]. To provide this apparatus with a proper performance at its maximum capability, all the resonant frequencies of the three elements must be matched as precisely as possible.

Most of the difficulty in building this device is associated to gauging the resonance frequencies towards matching. Because it is almost impossible to match all exactly, the audio amplifier must be strong enough to overcome any small difference in frequencies. Another fact that drives some attention is how to minimize the PZT effect in order to capture the bubble at the very center of the resonator, favoring a subsequent light emission.

For this matter, we performed some independent evaluations of the PZT behavior, measuring the impedance and the capacitance of each one separately and in parallel.

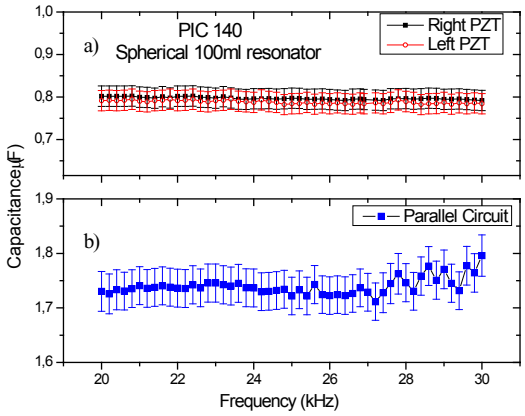

Figure 7 - The experimental measurements for the PIC 140 PZT attached to the 100ml spherical resonator: a) shows the capacitance value for the right and left PZT as a function of the frequency; b) reassess the capacitance x frequency relation for the parallel assembling of the PZT´s

In Figs. 7, 8 and 9, one can verify the behavior of the capacitance as a function of the frequency value. The capacitance remains almost constant for the pair of spherical resonators 100ml (PIC140 and PIC155) and 250ml (PIC 141). In Fig. 7 a) we perform a measure of capacitance for each - right and left - PZT independently. As depicted, their behavior is pretty the same inside the error bar, meaning that both are working properly. To verify if these values are in agreement, we can calculate the equivalent circuit for parallel capacitors C_1 and C_2 and we will obtain almost the same value as in b). In b), we measure two opposite side PZT´s together in parallel, and the resulting value, (1.70 ± 0.10) μF, is in good agreement with the theoretical prediction, as shown in table2.

For the plots presented in Fig. 8 a) and b) and Fig. 9 a) and b) we meet the same agreement with the corresponding theoretical values, as in Fig. 7 a) and b) respectively. The experimental data are also shown in table 2.

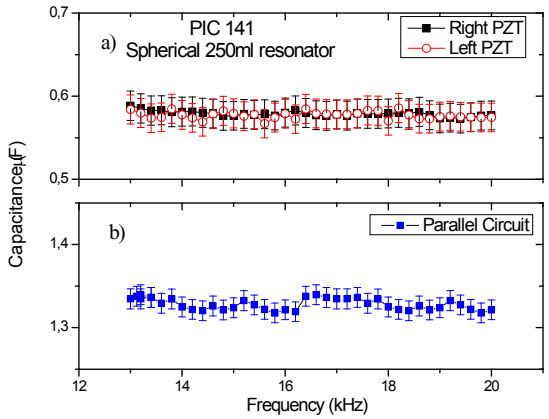

Figure 8 - The experimental measurements for the PIC 141 PZT attached to the 250ml spherical resonator

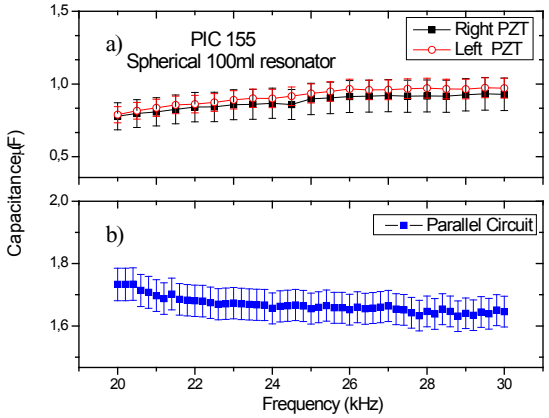

Figure 9 - The experimental measurements for the PIC 155 PZT attached to the 100ml spherical resonator. In a), the capacitance value for the right and left PZT varying with the frequency and in b) the measurement of both PZT´s together in parallel

In Fig. 10, the PZT´s of the cylindrical resonator show an unexpected behavior at lower frequencies, from (23.0 to 28.5) kHz, so in this region we won't be able to capture the bubble.

As the frequency increases we re-obtain the ordinary behavior as observed for the spherical resonators.

By means of these results we are able to identify the proper frequency range wherein our apparatus may allow for sonoluminescence.

To understand the variation of the impedance of the PZT attached to the resonators, we have to take into account that at very low frequencies, a circuit having a relatively low input capacitance and resistance has a input impedance almost equal to the input resistance: $Z \approx R$. Relatively low, here, means that the reactive part of the $Z = R/ (1+ i\omega RC)$ becomes small; that is, it holds that $RC << 1 / \omega$.

Whenever an input impedance of a circuit is considered, the output impedance of PZT must be taken into account [12]. For example, in this case, we know the PZT is of a capacitive nature, therefore, to define a frequency response of the input stage, sensor's capacitance must be connected in parallel with the circuit's input capacitance. Being the impedance a function of the signal frequency, the increase in the signal rate makes the input impedance decrease, as can be read from our experimental data displayed in the graphics of Figs. 11, 12 and 13. In a) we measured each PZT separately and in b), in parallel.

Through the analysis of these graphics at these frequencies range we verified that the predominant effect in those PZT's is capacitive.

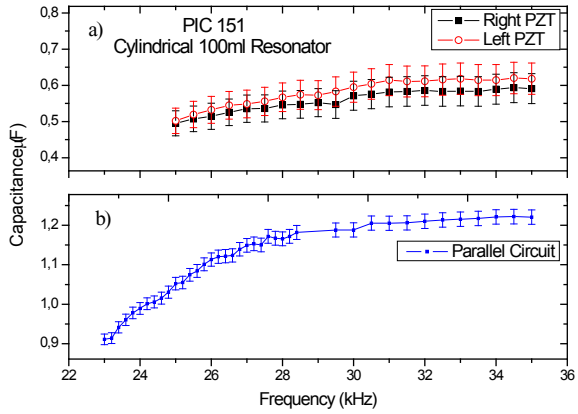

Figure 10 - The experimental measurements for the PIC 151 PZT attached to the 100ml cylindrical resonator. Again, a) presents the capacitance value for the right and left PZT varying with the frequency and b) shows the measurement for both PZT´s together in parallel. In a), the small frequencies effect is not as clearly stated as in b)

As for the cylindrical resonator impedance curve, Fig. 14, the predominant peak that appear in the graph is the point where it enters into the resonance mode (between 21 – 22 kHz), and then starts to decrease with the frequency as expected.

Table 2 - Experimental data for the impedance and capacitance measurements

Types of Resonators	Volume (ml)	Types of PZT	Theoretical Capacitance (nF)[b]	Experimental Capacitance (μF)[e]	Theoretical Inductance (μH)[c]	Experimental Inductance (μH)
Spherical	100	PIC140	1668.0	(1.73 ± 0.08)	0.23	(0.23± 0.05)
Spherical	250	PIC141	1355.2	(1.34 ± 0.08)	0.28	(0.28± 0.03)
Spherical	100	PIC155	1688.8	(1.71 ± 0.05)	0.23	(0.22± 0.10)
Cylindrical	100	PIC 151	1167.6	(1.19 ± 0.03)	0.33	(0.31± 0.10)

Values obtain using a linear fitting curve on the experimental data.

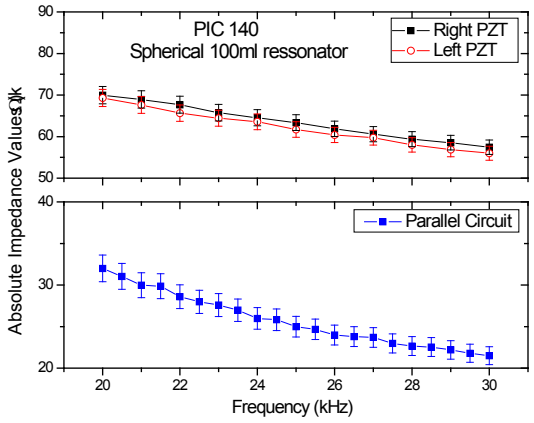

Figure 11 - The experimental measurements for the PIC 140 PZT attached to the 100ml spherical resonator. In a), one reads the absolute impedance value for the right and left PZT varying as a function of the frequency and in b) the corresponding measurement for the PZT´s in parallel is presented

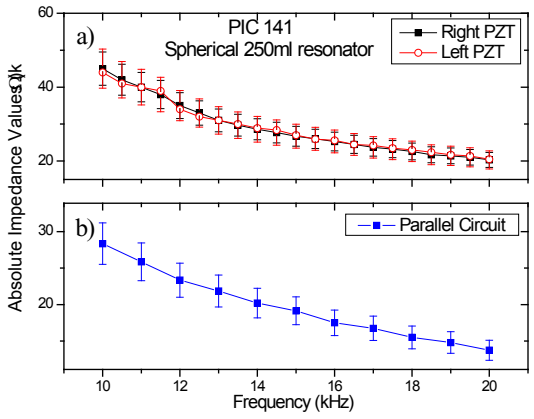

Figure 12 - The experimental measurements for the PIC 141 PZT attached to the 250ml spherical resonator. In a), the absolute impedance value for the right and left PZT varying with the frequency and in b) the corresponding measurement for PZT´s in parallel

6. SUMMARY AND REMARKS

All these studies were made to improve our SBSL apparatus performance at our Laboratory of Experimental Physics (LaFEA) and to analyze the behavior of the PZT´s according to the frequency to demonstrate the linearity of the components. Therefore, we could minimize our experimental errors in calculating the resonance frequency, eliminating losses in the circuit thereby; enabling a better fit of experimental setup, and improving the observation of the phenomenon of SL.

Future analyses are being performed to measure the quality factor, Q, of the resonators flasks. Q is a measure of tightness of the resonance and is given by the ratio of the frequency (f) at his maximum amplitude and Δ f that is the frequency spread at half power.

These measurements will give a good indication in what is missing in maintaining the emitting bubble light in the middle of the resonator, if the problem lies with the resonant chamber or with the electronics.

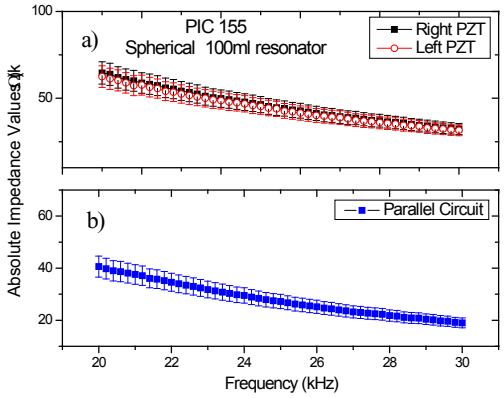

Figure 13 - The experimental measurements for the PIC 155 PZT attached to the 100ml spherical resonator. In a), the absolute

impedance value for the right and left PZT varying with the frequency and in b) the measurement for both PZT´s in parallel

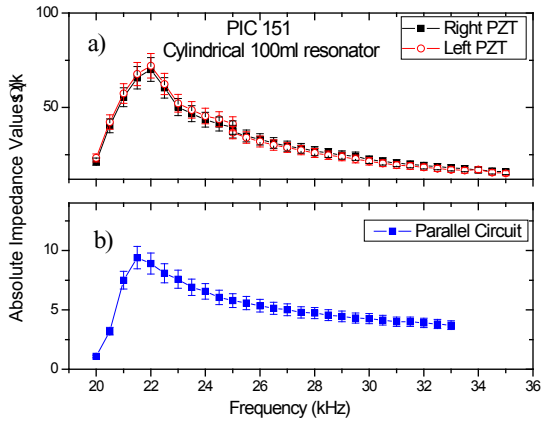

Figure 14 - The experimental measurements for the PIC 151 PZT attached at100ml cylindrical resonator. In a), the absolute impedance value for the right and left PZT varying with the frequency and in b) the measurement for both PZT´s in parallel

ACKNOWLEDGEMENTS

The authors would like to thank the Brazilian Federal CNPq agency and PIBIC-CEFET associated program for providing financial support for the co-authors that happen to be undergraduate-engineer students. And to FAPERJ Rio de Janeiro State Agency for funding some of the experimental equipments at LaFEA.

REFERENCES

[1] S. HILGENFELDT, „*Sonoluminescence: Sound basis for light emission*", Nature Physics **2**, 435 (2006).

[2] B.P. BARBER and S. J. PUTTERMAN: *"Light scattering measurements of the repetitive supersonic implosion of a sonoluminescing bubble*" Phys. Rev. Letts. **69**, 3839–42 (1992).

[3] K. S. SUSLICK, J. D. OXLEY, T. PROZOROV, "*Sonochemistry and Sonoluminescence of Room-Temperature Ionic Liquids"*, J. Am. Chem. Soc., **125**, 11138-39 (2003).

[4] D. J. FLANNINGAN et al., "*Measurement of Pressure and Density Inside a Single Sonoluminescing Bubble,*" Physical Review Letter, **96**, 204301 (2006).

[5] B. P. BARBER, R. A. HILLER, R. LöFSTEDT, S. J. PUTTERMAN, K. R. WENINGER: "*Alternative model of single-bubble sonoluminescence*", Phys. Rev. E **56**, 6750–6760 (1997).

[6] Channel Industries, Inc. 839 Ward Drive, Santa Barbara, CA, 93111 ciisales@channeltech.com.

[7] S. HATANAKA, et al., "*Relationship between a Standing-Wave Field and a Sonoluminescing Field"* Jpn. J. Appl. Phys. **38** 3053-3057 (1999).

[8] A. G.N. WATSON, *Treatise on the Theory of Bessel Functions*, Second Edition, Cambridge University Press. ISBN 0-521-48391-3. (1995)

[9] S.S. BAYIN, *Mathematical Methods in Science and Engineering*, Wiley, Chapter 2. (2006).

[10] A. M. BRODSKY, , L. W. BURGES and A. L. ROBINSON, "*Cooperative effects in sonoluminescence"* Physics Letters A, **287**, Issues 5-6, 3, 409-414 (2001).

[11] S. HILGENFELDT, D. LOHSE, and W. C. MOSS "*Water Temperature Dependence of Single Bubble Sonoluminescence*", Phys. Rev. Lett. **80**, 1332–1335 (1997).

[12] I. SINCLAIR and J. DUNTON, *Pratical Eletronic Handbook*, 6th edition, Newnes (2000).